Annu. Rev. Physiol. 2006. 68:375–401
doi: 10.1146/annurev.physiol.68.040104.134728

First published online as a Review in Advance on September 28, 2005

CNG AND HCN CHANNELS: Two Peas, One Pod

Kimberley B. Craven[1] and William N. Zagotta[1,2]
[1]*Department of Physiology and Biophysics, University of Washington, Seattle, WA 98195; email: kcraven@u.washington.edu*
[2]*Howard Hughes Medical Institute, University of Washington, Seattle, WA 98195; email: zagotta@u.washington.edu*

Key Words cyclic nucleotide, activation, gating, CNBD

■ **Abstract** Cyclic nucleotide–activated ion channels play a fundamental role in a variety of physiological processes. By opening in response to intracellular cyclic nucleotides, they translate changes in concentrations of signaling molecules to changes in membrane potential. These channels belong to two families: the cyclic nucleotide–gated (CNG) channels and the hyperpolarization-activated cyclic nucleotide–modulated (HCN) channels. The two families exhibit high sequence similarity and belong to the superfamily of voltage-gated potassium channels. Whereas HCN channels are activated by voltage and CNG channels are virtually voltage independent, both channels are activated by cyclic nucleotide binding. Furthermore, the channels are thought to have similar channel structures, leading to similar mechanisms of activation by cyclic nucleotides. However, although these channels are structurally and behaviorally similar, they have evolved to perform distinct physiological functions. This review describes the physiological roles and biophysical behavior of CNG and HCN channels. We focus on how similarities in structure and activation mechanisms result in common biophysical models, allowing CNG and HCN channels to be viewed as a single genre.

INTRODUCTION

Ion channels are molecular machines that enable cells to communicate with the extracellular world (1). These allosteric proteins permit ions to flow into or out of cells through a conducting pore, thus allowing the cells to regulate their membrane potentials and intracellular Ca^{2+} concentrations in response to intracellular or extracellular events. The process of gating, the opening and closing of an ion-permeable pore, can be initiated by changes in membrane voltage, binding of ligands, or changes in membrane stretch due to mechanical stimuli, depending on the type of ion channel. This review focuses on similarities and differences between two families of ion channels that are gated by binding of cyclic nucleotide ligands: the cyclic nucleotide–gated (CNG) channels and the hyperpolarization-activated cyclic nucleotide–modulated (HCN) channels. CNG channels are nonselective cation channels that are activated very weakly by membrane depolarization. HCN channels are weakly K^+-selective cation channels that are activated by membrane

hyperpolarization. Both channels, however, are activated by cyclic nucleotide binding, which produces a large increase in current in CNG channels and a depolarizing shift in the voltage dependence of activation for HCN channels. These electrophysiological properties tune each of these channels to different physiological roles.

PHYSIOLOGICAL ROLES

CNG Channels

Cyclic nucleotide–gated (CNG) channels generate the primary electrical signal in photoreceptors and olfactory sensory neurons. CNG channels are nonselective cation channels that are opened, or gated, by direct binding of intracellular cyclic nucleotides (2–4). In vertebrate rod photoreceptors, CNG channels open in response to guanosine 3′,5′-cyclic monophosphate (cGMP) binding. In the dark, CNG channels conduct a steady inward current (consisting primarily of Na^+ and Ca^{2+}) as a component of the dark current. Light striking the retina activates the phototransduction cascade on the disc membranes of rod photoreceptor outer segments (Figure 1) (5). Photoactivated rhodopsin activates phosphodiesterase via

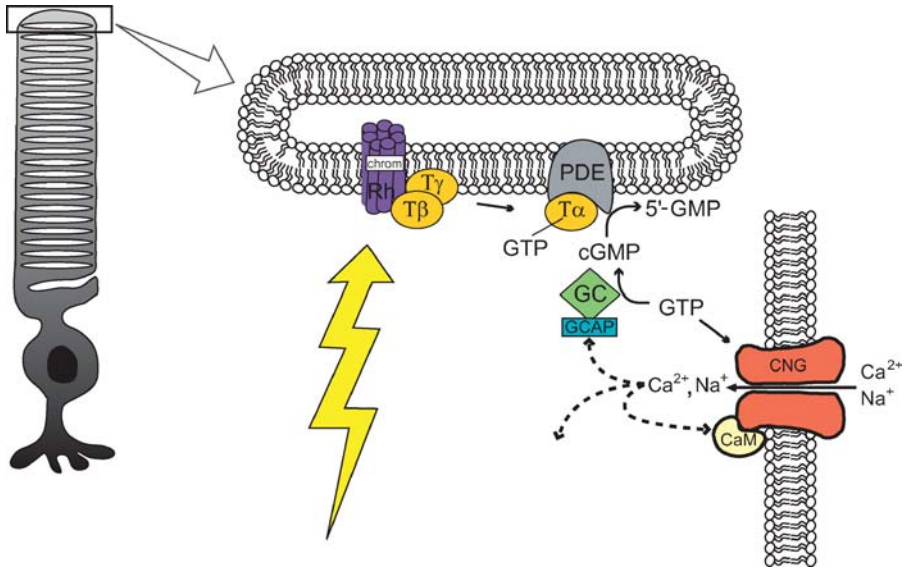

Figure 1 Phototransduction cascade in rod photoreceptor. Rod photoreceptor (*left*) with phototransduction cascade on rod disc membrane and rod outer segment (*right*). A photon activates rhodopsin (Rh), which in turn activates the heterotrimeric G protein transducin (T), whose α subunit activates a phosphodiesterase (PDE). A CNG channel is shown in the outer segment membrane, and the downstream effects of Ca^{2+} influx [calmodulin (CaM) binding, activation of guanylyl cyclase (GC) by guanylyl cyclase–activating protein (GCAP), and other effects] are shown with dotted arrows.

the GTP-binding protein transducin. The phosphodiesterase hydrolyzes cGMP into 5′-GMP, leading to the closure of CNG channels and a decrease in inward current. This hyperpolarizes the outer segment and terminates the tonic release of neurotransmitter that occurs in the dark when cGMP levels are high and CNG channels are open. Therefore, it is the termination of a neurotransmitter signal to the downstream retinal cells and neurons that indicates detection of a photon. The decrease in Ca^{2+} influx also has an important downstream effect: It is detected by Ca^{2+}-sensing proteins such as guanylyl cyclase–activating protein (GCAP), which stimulates guanylyl cyclase, resulting in the increase of cGMP production from GTP (6–8).

CNG channels also play a crucial role in olfactory signal transduction. In olfactory sensory neurons, binding of an odorant to an olfactory receptor activates adenylate cyclase, which produces an increase in the intracellular concentration of adenosine 3′,5′-cyclic monophosphate (cAMP) (Figure 2). This increase in intracellular cAMP leads to opening of CNG channels, which depolarizes the olfactory sensory neurons. Depolarization results in the release of neurotransmitter, signaling to downstream neurons that an odorant has been detected (9). As in phototransduction, Ca^{2+} influx is likewise important in olfactory transduction. Ca^{2+} activates calmodulin, which can bind to and inhibit olfactory CNG channels, a process proposed to underlie olfactory adaptation (10–13). Additionally,

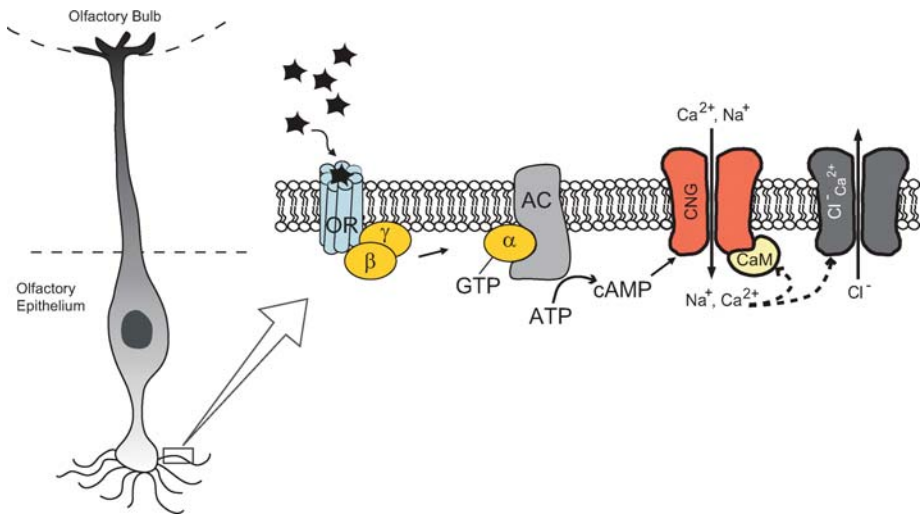

Figure 2 Olfactory transduction cascade in olfactory epithelium. Olfactory receptor cell (*left*) with olfactory transduction cascade in cilia (*right*). Odorants bind to and activate the olfactory receptor (OR), which activates a heterotrimeric G protein, whose α subunit activates adenylyl cyclase (AC). AC produces cAMP, which activates CNG channels. Downstream effects of Ca^{2+} [binding of calmodulin (CaM) and activating of a Ca^{2+}-sensitive Cl^- channel] are shown by dotted arrows.

Ca^{2+} activates Ca^{2+}-sensitive Cl^- channels to amplify this response. CNG channels are also located in other sensory tissues—such as taste receptors, and nonsensory tissues such as the hippocampus, heart, testis, kidney, pancreas, adrenal gland, and colon—in which their roles are not as well understood as in phototransduction and olfaction (3, 4).

There are six vertebrate CNG channel subunits: CNGA1, CNGA2, CNGA3, CNGA4, CNGB1, and CNGB3. These subunits can assemble in a variety of combinations to produce tetrameric channels. Three of these subunit types, CNGA1, CNGA2, and CNGA3, can form homomeric channels in heterologous expression systems. CNGA4, CNGB1, and CNGB3 do not form functional homomeric channels but can coassemble with other subunits to form functional heteromeric channels. In fact, most native channels are thought to be composed of more than one subunit type. For example, CNG channels of rod photoreceptors contain three CNGA1 subunits and one CNGB1 subunit (14–16). Those of cone photoreceptors are also heteromeric and are thought to form from two CNGA3 and two CNGB3 subunits (17). CNG channels of olfactory neurons have been proposed to be composed of two CNGA2 subunits, one CNGA4 subunit, and one alternatively sliced CNGB1 subunit, CNGB1b (18). The assorted combinations of these six subunits give each tissue-specific CNG channel unique properties to perform its physiological role.

HCN Channels

Hyperpolarization-activated cyclic nucleotide–modulated (HCN) channels constitute a related family of channels with a very different physiological role from CNG channels. HCN channels regulate neuronal and cardiac firing rates. HCN channels are cation channels that are modulated by binding of cyclic nucleotides, like CNG channels. Unlike CNG channels, however, they are activated by membrane hyperpolarization and are weakly selective for potassium. The current generated by HCN channels has been called the I_h (hyperpolarization), I_q (queer), or I_f (funny) current; one area in which it has been described extensively is the cardiac sinoatrial node (19–21). The sinoatrial node is the pacemaker region of the heart, and currents through several types of ion channels cooperate in order to generate spontaneous rhythmic firing of cardiac action potentials (Figure 3) (22, 23). HCN channels are activated by membrane hyperpolarization after a cardiac action potential. When activated, HCN channels conduct inward current and depolarize the cell toward the threshold of voltage-gated calcium channel activation, which in turn leads to firing of another cardiac action potential. In this manner, rhythmic firing is generated (21, 24). Neurotransmitters, such as norepinephrine, or pharmacological agents, such as a β-adrenergic agonist, can elevate cAMP levels and produce an accelerated heart rate (25, 26) This is due, in part, to the binding of cAMP to HCN channels, shifting the voltage dependence of activation to more depolarized potentials and increasing both the rate of channel opening and the maximal current level.

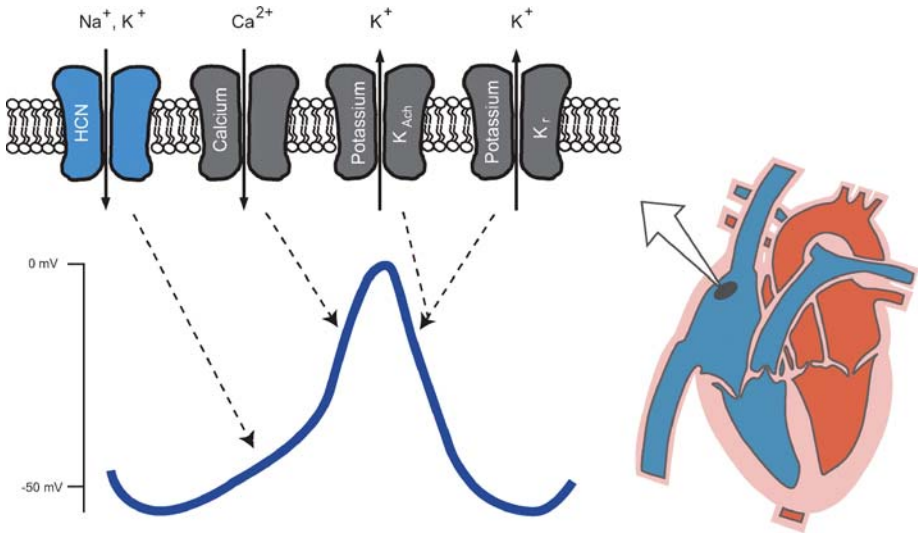

Figure 3 Heart sinoatrial node pacemaker current. Sinoatrial node (*black oval*) of the heart (*right*) and the ion channels responsible for pacemaker activity (*left*). Each channel contributes to a phase of the sinoatrial action potential, indicated by the dotted arrows.

HCN channels also mediate pacemaker activity in the nervous system by a similar mechanism as in the heart, although the gating kinetics in the nervous system must be faster than in the heart, as neuronal action potentials are faster than cardiac action potentials (27, 28). Neurons in the globus pallidus of the basal ganglia exhibit tonic activity whose rate and regularity are attributed to HCN channels (29). Moreover, as in the heart, cAMP speeds the activation kinetics and maximal current levels of HCN channels in the nervous system, and neurotransmitters can influence firing rates by either increasing or decreasing cAMP levels (30–33).

Besides acting as a pacemaker, HCN current also functions as a regulator of resting potential and membrane resistance. Moreover, HCN channels regulate synaptic transmission and contribute to nervous system development. In both neurons and muscle cells, HCN channels are activated at rest, and the inward sodium current leads to slightly depolarized resting potentials (34). HCN current stabilizes the resting membrane potential because small hyperpolarizations activate HCN channels, whose inward current depolarizes the cell. This depolarization deactivates HCN channels, preventing further departure from the resting potential. In retinal photoreceptors, hyperpolarization during bright light activates HCN channels, and the HCN current returns the membrane potential closer to depolarized levels as in the dark, allowing for adaptation of synaptic transmission during bright light (34). It has been suggested that I_h controls the spontaneous oscillatory activity during development that is required for neural network maturation. One example of this is in the cerebellum, in which HCN channels are expressed early in development in

basket cells. Basket cells are inhibitory GABAergic cells that modulate Purkinje cell behavior (35). This HCN activity has also been shown to affect membrane resistance and dendritic integration (36, 37).

The HCN channel family, like the CNG channel family, comprises several subunit types. There are four known HCN subunit isoforms, HCN1–HCN4, which combine to form tetrameric channels in the heart and the nervous system. HCN1 is expressed in photoreceptors, dorsal root ganglia, cortex, cerebellum, and sinoatrial node. HCN2 is expressed in the sinoatrial node, dorsal root ganglia, and basal ganglia. HCN3 is widely expressed in the brain, but at low levels. HCN4 is expressed in the sinoatrial node and subcortical areas (38, 39). Although each subunit can form homomeric channels in heterologous expression systems, the subunits combine in diverse ways to form heteromeric channels in the heart and brain of different species. For example, HCN1 and HCN4 subunits have been proposed to form HCN channels in the rabbit sinoatrial node, whereas HCN2 and HCN4 subunits are thought to form HCN channels in the mouse sinoatrial node (23, 40). In the mouse brain, HCN channels of globus pallidus appear to be composed of the HCN1 and HCN2 subunits (29). Currently, the subunit stoichiometry of these native channels is unknown.

SIMILARITY IN STRUCTURES OF CNG AND HCN CHANNELS

Despite their different physiological roles, CNG and HCN channels are closely related in structure. Both channels belong to the superfamily of voltage-gated potassium (K^+) channels and are thought to be tetrameric proteins whose subunits are arranged around a central pore. Each subunit has six transmembrane domains and intracellular N and C termini (Figure 4). The fourth transmembrane domain (S4) contains several positively charged amino acids, as in K^+ channels. The HCN S4 functions as a voltage sensor, and the CNG S4 can function as a voltage sensor if placed in a permissive structural environment, such as the ether-a-go-go (Eag) K^+ channel (41). The pore region comprises the fifth transmembrane domain (S5), a reentrant pore loop that does not completely traverse the membrane, and the sixth transmembrane domain (S6). As with voltage-gated K^+ channels, the pore regions of CNG and HCN channels are thought to be similar to that of KcsA, the potassium channel from *Streptomyces lividans* whose crystal structure has been solved (42). The intracellular N-terminal regions are divergent in the various HCN and CNG subunits, and in CNG channels, the N terminus can be autoexcitatory and contribute to calmodulin modulation (43). Contained within the intracellular C termini of both HCN and CNG channels is a ligand-binding domain called the cyclic nucleotide–binding domain (CNBD). The CNBD is connected to the end of the S6 by the C-linker. Binding of ligand to the CNBD favors channel opening in both CNG and HCN channels, perhaps owing to a conformational change in the CNBD, which may be conferred to the pore through movement in the C-linker. The

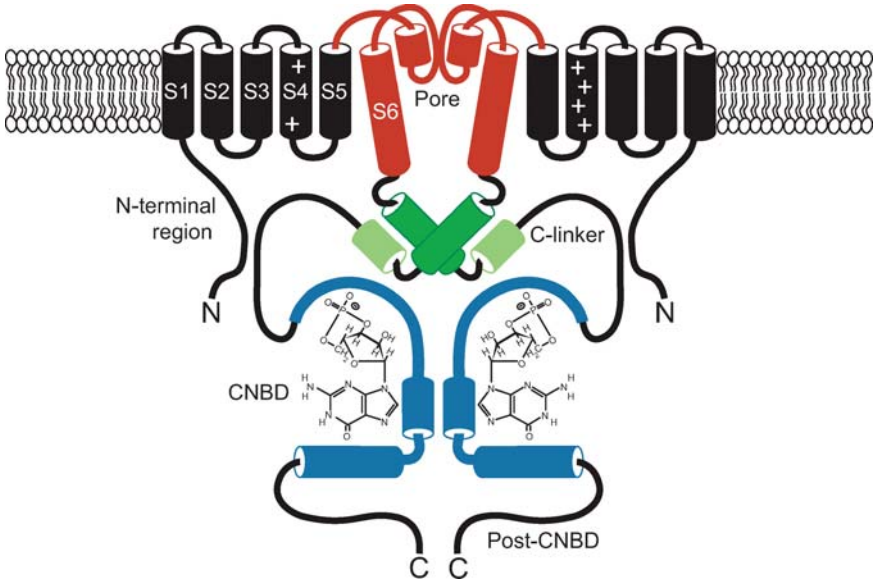

Figure 4 Membrane topology of CNG and HCN channels. Two of the four subunits of a CNG or HCN channel are shown. The transmembrane segments (S1–S6) are shown in black, except for the pore region (S6 and pore loop), which is shown in red. The voltage sensor (S4) is indicated by positive charges. The C-terminal region contains the cyclic nucleotide–binding domain (CNBD, *blue*, shown with cGMP bound) and the C-linker (*green*), which connects the CNBD to the pore.

region of C terminus past the CNBD, called the post-CNBD region, is proposed to be important in subunit assembly of CNG channels (16, 44).

The CNG and HCN channels exhibit high sequence similarity to two other channel families, Eag-like K^+ channels and plant K^+ channels, as illustrated by a phylogenetic tree (Figure 5). Like CNG and HCN channels, these channels also contain C-linkers and CNBDs (Figure 6), although the effects of cyclic nucleotides on these channels are weak or disputed (45–47). The difference in cyclic nucleotide modulation may be due to a lack of conservation in key residues involved in cyclic nucleotide coordination. This suggests that the fold of the CNBDs may serve other functions for these channels, such as binding other signaling molecules.

BIOPHYSICAL PROPERTIES OF CNG AND HCN CHANNELS

Permeability

Under physiological conditions, CNG channels carry an inward Na^+ and Ca^{2+} current. CNG channels are nonselective cation channels, allowing the monovalent

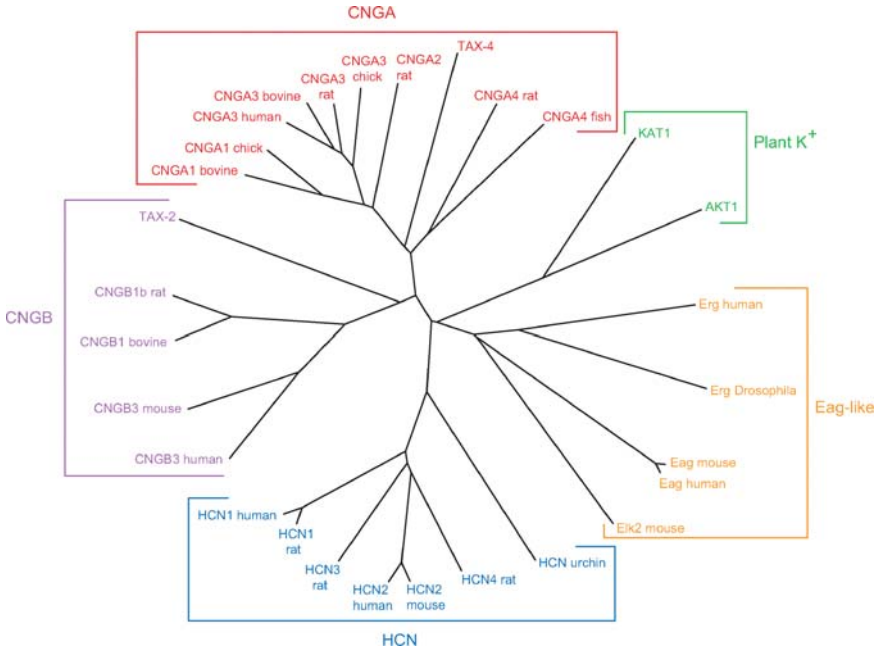

Figure 5 Unrooted phylogenetic tree showing relationships of the CNG, HCN, plant K^+, and ether-a-go-go (Eag)-like K^+ channel families. CNGA channel members (*red*): CNGA1 (formerly CNG1), CNGA2 (formerly CNG2), CNGA3 (formerly CNG3), CNGA4 (formerly CNG5), and TAX-4 (*Caenorhabditis elegans*). CNGB channel members (*purple*): CNGB1 (formerly CNG4), CNGB3 (formerly CNG6), and TAX-2 (*C. elegans*). HCN channel members (*blue*): HCN1 (formerly HAC2), HCN2 (formerly HAC1), HCN3 (formerly HAC3), HCN4 (formerly HAC4), and urchin HCN (also known as SpIH or spHCN). Eag-like channel members (*yellow*): Eag, Elk, ether-a-go-go-related gene (Erg), and human Erg, also known as HERG. Plant K^+ channel members (*green*): KAT1, AKT1. Sequences aligned with ClustalW, www.ebi.ac.uk/clustalw/, and tree drawn with PHYLIP software array, http://evolution.genetics.washington.edu/phylip.html.

cations K^+, Na^+, Li^+, Rb^+, and Cs^+ to conduct almost equally well (3). Although divalent cations can permeate the channel, at high concentrations they also block the channel. These permeability properties most closely resemble that of voltage-dependent Ca^{2+} channels and are due, in part, to an acidic residue in the outer mouth of CNG channels (48–52). This acidic residue replaces the YG of the GYG signature sequence in the pore loop of K^+ channels (53).

In contrast to the nonselective cation selectivity of CNG channels, HCN channels are more permeable to K^+ than Na^+ (with permeability ratios of about 4:1) and are blocked by millimolar concentrations of Cs^+ (54, 55). Despite this preference for K^+ conductance, perhaps conferred by the GYG motif in the pore loop,

HCN channels also carry an inward Na^+ current under physiological conditions (56). HCN channels can also conduct Ca^{2+}, but not as well as CNG channels. For example, with 2.5 mM external [Ca^{2+}], the fractional Ca^{2+} current of HCN4 is 0.6%, whereas for CNGA3 it is 80% (57, 58). Unlike CNG channels, HCN channels are not blocked by divalent cations (59).

Voltage Dependence

An important difference between these two channel families is their degree of voltage dependence (Figure 7). As indicated above, the S4 of both CNG and HCN channels contains positively charged residues, as do the voltage-dependent K^+ channels that activate with depolarization. Surprisingly, however, HCN and CNG channels both behave differently from K^+ channels: HCN channels are activated by hyperpolarization and CNG channels are practically insensitive to voltage. S4s of both HCN and K^+ channels seem to respond similarly to changes in membrane potential, as they are accessible from the inside upon hyperpolarization and accessible from the outside upon depolarization (60, 61). The difference between HCN and K^+ channels is thought to be in the coupling to opening: HCN channels open with hyperpolarization whereas K^+ channels open with depolarization. It has also been proposed that, instead of merely having an opposite coupling mechanism, HCN channels couple voltage sensing to channel activation through a novel mechanism of transmembrane rearrangement (62). HCN channels are moderately voltage sensitive, on the average moving the equivalent of six electric charges through the membrane with activation, compared to thirteen electric charges for *Shaker* K^+ channels (63–65). The other subtypes of HCN channels have charge movements ranging from four to six electric charges (34, 54, 66–74). In addition to being activated by hyperpolarization instead of depolarization, HCN channels are also activated more slowly (0.2–2 sec) than most potassium channels. The voltage-activated gate has been shown to be on the intracellular side of the channel (75, 76).

Modulation of CNG and HCN Channels by Cyclic Nucleotides

A unifying biophysical property of CNG and HCN channels is their modulation by cyclic nucleotides. For both CNG and HCN channels, binding of cyclic nucleotides to the CNBD favors channel opening. The C-terminal regions of both channel families have high sequence similarity, suggesting perhaps that HCN and CNG channels sense and report ligand binding in similar ways (see Figure 6 for sequence alignment). This is supported by the fact that mutations in the CNBD regions of both CNG and HCN channels appear to have similar effects. For example, the same basic residue, Arg559 (CNGA1), Arg591 (HCN2), and Arg538 (HCN1), appears to interact with ligand in all three channels (66, 77, 78). If this Arg is mutated to an acidic amino acid, such as Glu, the channel retains normal kinetic and voltage behavior but binds cyclic nucleotides weakly. For HCN channels, the mutant channel no longer exhibits a shift in voltage dependence with cAMP, and for CNG channels, the mutant channel has a 1000-fold reduction in ligand affinity.

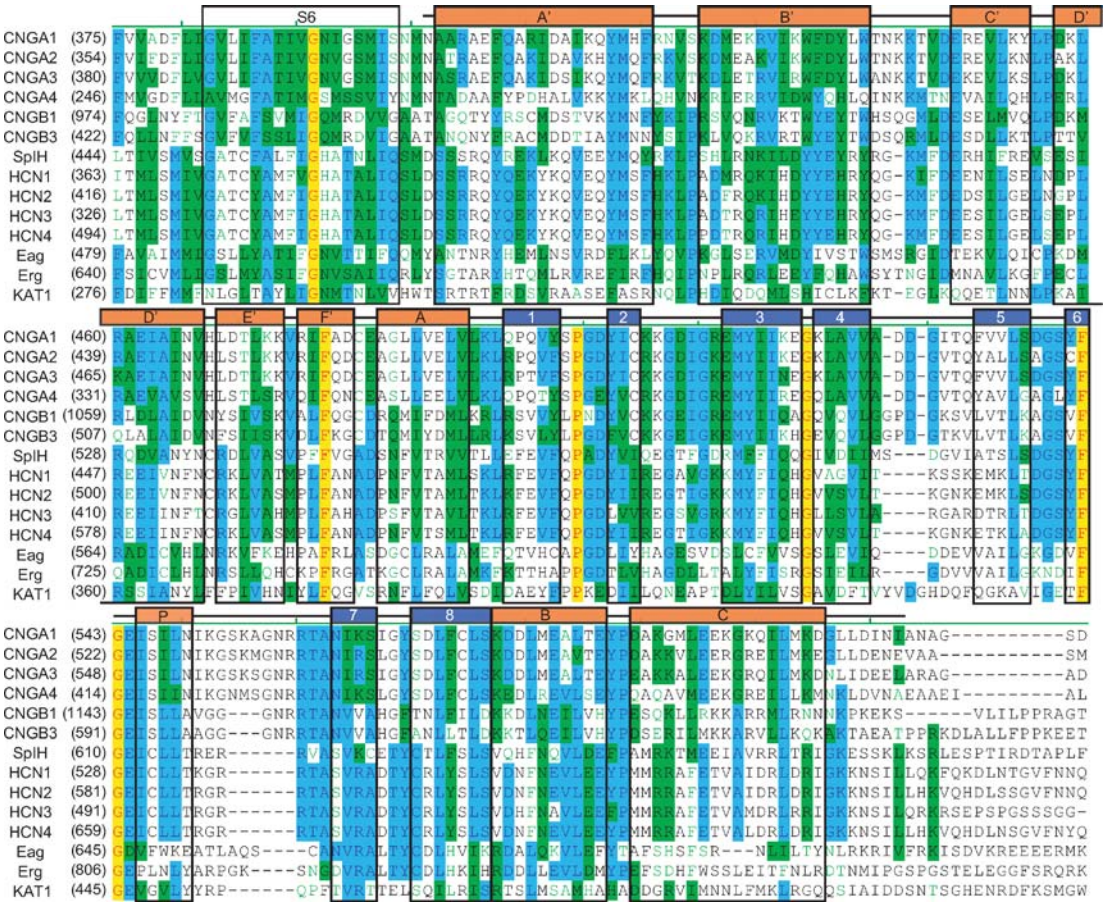

Another indication of the similarity in CNG and HCN C termini is that the same salt bridges exist in the C-linkers of both channels (67). These experiments suggest that CNG and HCN channels interact with ligand in the same way and then undergo similar conformational changes.

HCN2 C-TERMINAL CRYSTAL STRUCTURE Recently, the crystal structure of the C-terminal region was solved for the HCN2 channel (73), shedding light on how cyclic nucleotides bind and how this binding may lead to channel opening. The crystal structure begins just after the end of S6 and extends through the C-linker and CNBD but does not include the post-CNBD region. The structure is a tetramer with a fourfold axis of symmetry and a hole down the central axis (Figure 8). The C-terminal region of HCN and CNG channels is thought to hang below the pore, like the "hanging gondola" of voltage-gated K^+ channels (79, 80). Although electronegative in character, the hole down the central axis has been shown not to be an obligatory part of the ion pathway (81). The top portion of the structure consists of the C-linkers, six α-helices (A′–F′), with the N terminus of each C-terminal fragment located close to each other on the very top of the structure (Figure 8). The bottom portion of the structure consists of the CNBDs, each of which demonstrates the same fold as the CNBD of other cyclic nucleotide–binding proteins such as catabolite gene activator protein (CAP) and cAMP-dependent protein kinase (PKA) (82, 83). Each CNBD contains an α-helix (A), followed by a β-roll formed by eight β-strands (1–8), followed by two α-helices (B and C). There is also an additional short α-helix, called the P-helix, between β-strands 6 and 7.

Most of the intersubunit contacts in the HCN2 C-terminal region crystal structure are in the C-linker region. The C-linker of each subunit contains six α-helices, and the first two helices (A′ and B′) form an antiparallel helix-turn-helix motif that interacts with the second two helices (C′ and D′) of the neighboring subunit (Figure 8). This interacting region has been likened to an "elbow on a shoulder," in which the "elbow" is the A′ and B′ helix-turn-helix motif that rests on the "shoulder," the C′- and D′-helices of the neighboring subunit. The interaction

←

Figure 6 Sequence alignment of CNG, HCN, and related families. Sequence alignment includes all members of the CNG channel family (bovine CNGA1, rat CNGA2, human CNGA3, rat CNGA4, bovine CNGB1, and human CNGB3) and HCN channel family (rat HCN1, mouse HCN2, rat HCN3, and rat HCN4) as well as SpIH (sea urchin HCN), two members of the Eag-like channels (mouse Eag and human Erg), and one plant K^+ channel (KAT1). The tertiary structure elements—the last transmembrane sequence (S6) as well as the α-helices of the C-linker (A′–F′) and the β-sheets (1–8) and α-helices (A–C, P) of the CNBD—are boxed (α-helices are in *orange boxes* and β-sheets in *indigo boxes*). The HCN2 C-terminal crystal structure extends from Asp443 to Leu643 (HCN2 amino acid numbers).

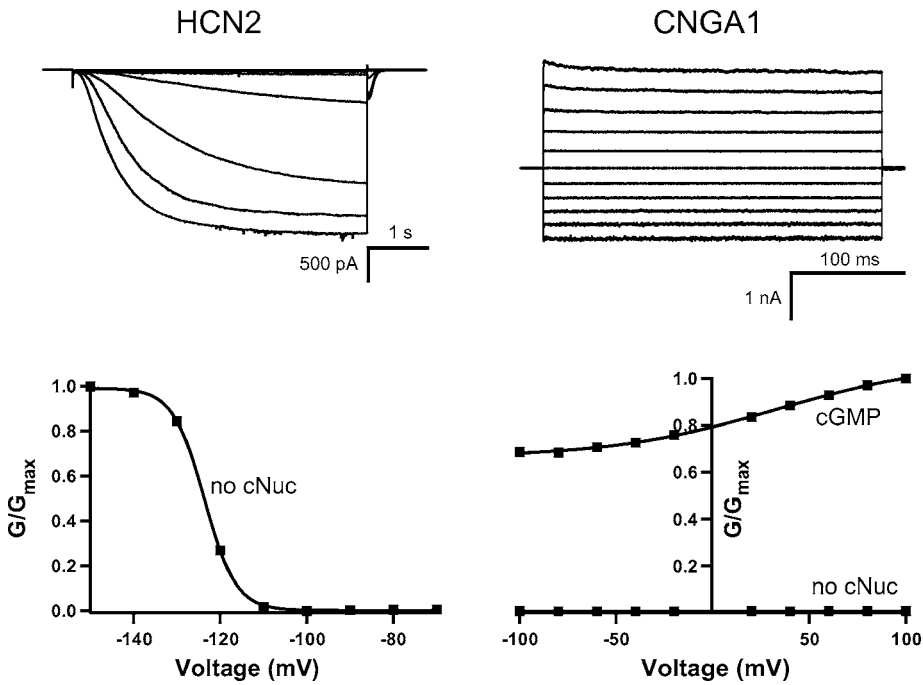

Figure 7 Voltage dependence of HCN2 and CNGA1. Behavior of HCN2 (*left*) and CNGA1 (*right*) channels in response to voltage. HCN2 currents (*left*, *top*) were recorded in response to voltage pulses from a holding potential of 0 mV to test potentials between −70 mV and −150 mV, returning to a tail potential of −40 mV. The conductance-voltage relation (*left*, *bottom*) was obtained from normalized tail currents. CNGA1 currents (*right*, *top*) were recorded in the presence of saturating cGMP and were recorded in response to voltage pulses from a holding potential of 0 mV to test potentials between −100 mV to +100 mV. The conductance-voltage relations with and without cGMP (*right*, *bottom*) were calculated from the currents and the driving force.

between the "elbow" and the "shoulder" involves hydrogen bonds, hydrophobic interactions, and salt bridges.

The C-terminal region of HCN2 was crystallized in the presence of two different ligands, cAMP and cGMP. The structures of the different ligand-bound channels were virtually identical, only differing in the configuration of the cyclic nucleotide itself. cAMP binds between the β-roll and the C-helix in the anti configuration, the configuration with the purine ring rotated away from the phosphoribose (Figure 9). Arg591 of the β-roll electrostatically interacts with the phosphate of cAMP. This has also been demonstrated in electrophysiology experiments, in which mutating this Arg to a Glu results in a large decrease in HCN2 affinity for cAMP (66). The β-roll and P-helix also interact with oxygens on the phosphoribose through hydrogen bonding. Additionally, the purine ring of cAMP interacts with Arg632 and Ile636

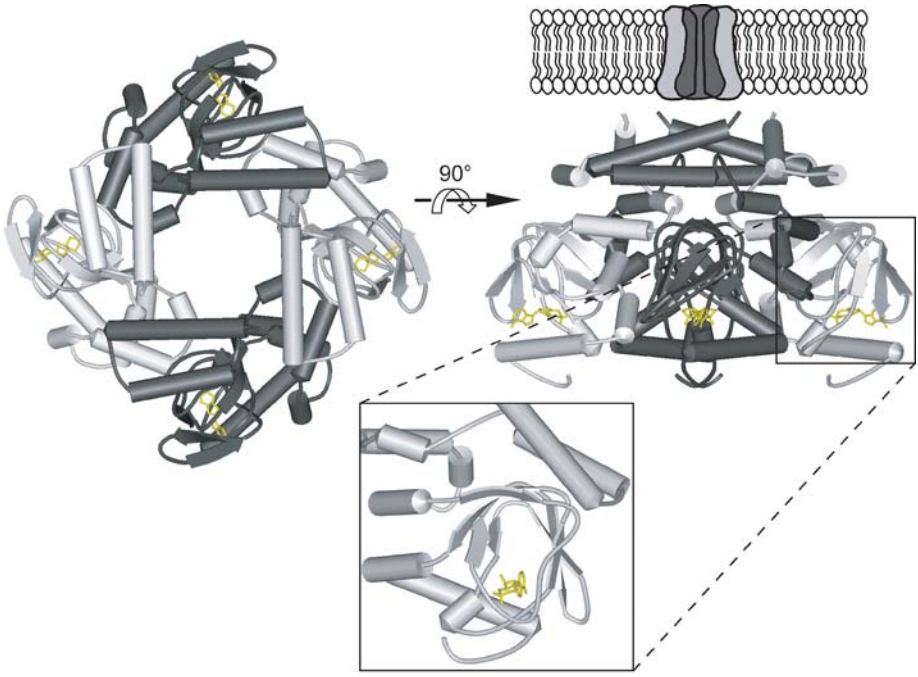

Figure 8 HCN2 C-terminal crystal structure. Structure of the HCN2 C-terminal region (73), viewed from the membrane (*left*) and from the side (*right*). The structure is positioned below the membrane-spanning portion of the channel, as it is thought to be in vivo. The structure contains four subunits, two in dark gray and two in light gray, with the C-linkers comprising the top half of the structure and the CNBDs the bottom half. cAMP (*yellow*) is bound in the CNBD of each subunit. The inset shows an enlargement of the β-roll of the CNBD, where cAMP binds.

of the C-helix. The phosphoribose of cGMP binds in the identical position, but cGMP binds in the syn configuration, the configuration with the purine ring folded back on top of the phosphoribose (Figure 9). In the syn configuration, the purine ring of cGMP can hydrogen bond with Thr592 of the β-roll. This interaction is also thought to occur in CNG channels, where Thr560 of rod channels and Thr537 of olfactory channels appear to confer cGMP selectivity. Mutation of these Thr residues decreases the channels' apparent affinity for cGMP while barely affecting cAMP affinity (84). The HCN2 C-terminal crystal structure not only provides insight into how the C-terminal regions of CNG and HCN channels are arranged and how ligands bind to the CNBD but also provides a framework for understanding biophysical data concerning cyclic nucleotide modulation.

EFFECTS OF CYCLIC NUCLEOTIDES ON HCN CHANNELS HCN channels are activated by both membrane hyperpolarization and cyclic nucleotide binding. Voltage

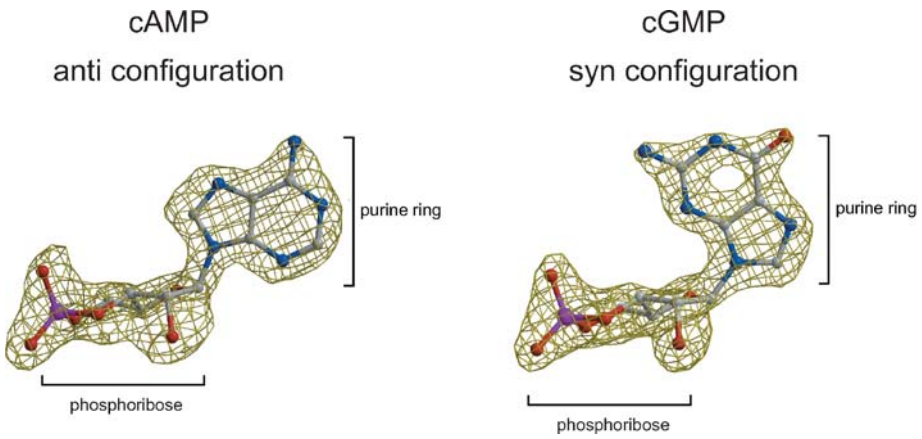

Figure 9 Cyclic nucleotide crystal structures. Density from X-ray crystallography (*web-bing*) shown for cAMP (*left*) and cGMP (*right*), with the chemical structure of the molecules shown in ball-and-stick format. Elements are coded with color: carbon (*gray*), nitrogen (*blue*), phosphorous (*purple*), hydrogen (*red*).

and cyclic nucleotides, in fact, appear to activate the channel via the same gate (75, 76, 85). For homomeric HCN2 channels, saturating concentrations of both cAMP and cGMP produce the same effects. They both increase open probability at hyperpolarizing voltages, speed activation kinetics, and shift the voltage dependence of activation to more depolarized voltages (54). In response to hyperpolarization, HCN2 channels open with a predominantly exponential time course after an initial lag, with a midpoint of voltage activation (V_{half}) of approximately −130 mV (Figure 10). Saturating concentrations of cAMP shift the voltage dependence of activation approximately 15 mV in the depolarized direction (V_{half} of approximately −115 mV), speed the activation kinetics, and increase the maximal current at hyperpolarized voltages (67, 71, 73, 74). cAMP stabilizes the open state relative to the closed state, as measured by the change in free energy (ΔG) of channel opening in the presence of cAMP relative to the ΔG in the absence of ligand, $\Delta\Delta G$. The $\Delta\Delta G$ for HCN2 channels in the presence of cAMP is approximately −3 kcal mol^{-1} (73). Saturating cGMP produces a similar effect on HCN2 channels, shifting the activation curve approximately the same amount but not speeding the activation kinetics quite as much (54, 73, 85). However, these cGMP effects require a 10-fold higher concentration of agonist to produce the same shift as cAMP. This cyclic nucleotide specificity probably results from hydrogen bonding between Arg632 in the C-helix and the purine ring of cAMP as well as from hydrophobic interactions between the adenine ring and the binding pocket. Despite differences in affinity, both cyclic nucleotides stabilize the closed-to-open equilibrium for HCN2 channels, enabling activation with less hyperpolarization and more complete activation at hyperpolarized voltages. Other HCN isoforms are similarly modulated by cAMP, exhibiting depolarizing shifts in V_{half} and accelerated activation

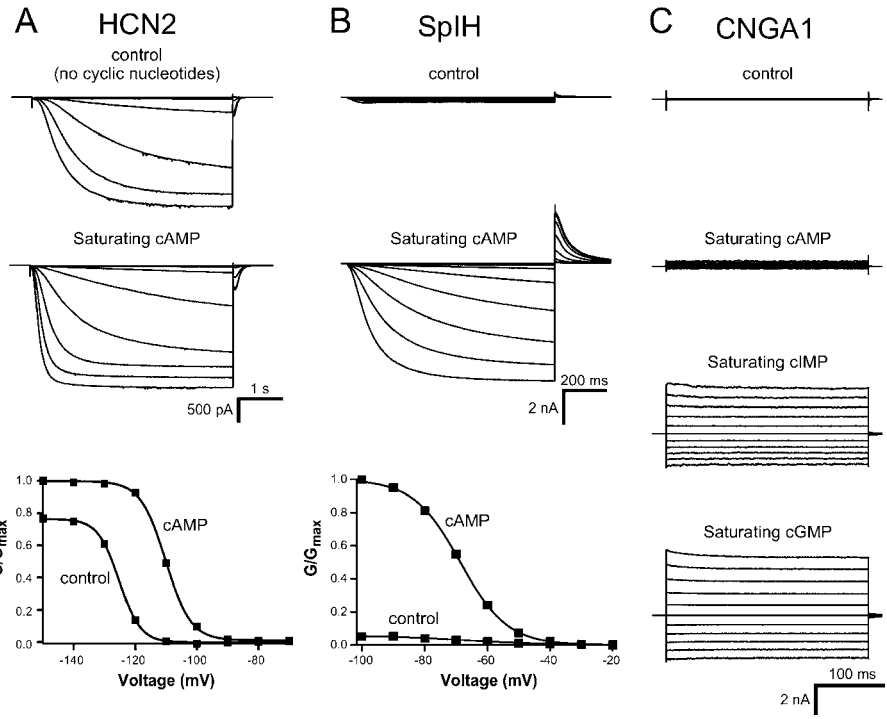

Figure 10 Cyclic nucleotide dependence of HCN2, SpIH, and CNGA1. Behavior of HCN2 (*A*), SpIH (*B*), and CNGA1 (*C*) channels in response to cyclic nucleotides. (*A*) HCN2 currents were recorded in the absence (*top*) or presence (*middle*) of saturating cAMP in response to voltage pulses from a holding potential of 0 mV to test potentials between –70 mV and –150 mV, returning to a tail potential of –40 mV. The conductance-voltage relations (*bottom*) were obtained from normalized tail currents. (*B*) SpIH currents were recorded in the absence (*top*) or presence (*middle*) of saturating cAMP in response to voltage pulses from a holding potential of 0 mV to test potentials between –20 mV and −100 mV, returning to a tail potential of +40 mV. The conductance-voltage relations (*bottom*) were obtained from normalized tail currents. (*C*) CNGA1 currents were recorded in the absence (*top*) and presence of saturating cAMP, cIMP, and cGMP in response to voltage pulses from a holding potential of 0 mV to test potentials between −100 mV to +100 mV.

kinetics, but they are not all modulated to the same degree. HCN1 channels display a shift in V_{half} of merely 2–5 mV in the presence of cAMP, whereas HCN4 channels shift approximately 15 mV (24, 71, 74).

A related HCN channel, SpIH (also known as spHCN) is found in sea urchin sperm. SpIH is a cation channel that, like other HCN channels, favors K^+ conductance and is responsive to both hyperpolarization and cAMP binding (86). The sequence of the SpIH subunit is most similar to that of the mammalian HCN channels (Figure 5). However, SpIH behavior differs from that of the rest of the HCN subunits

in one noteworthy way: In the absence of cyclic nucleotide, hyperpolarization-activated currents inactivate (Figure 10). Binding of cAMP eliminates inactivation and dramatically increases the probability of opening with no shift in voltage dependence. SpIH channels are moderately voltage sensitive, moving approximately five equivalent charges through the membrane with activation, with a V_{half} of approximately −80 mV (76, 86). As in HCN channels, both voltage and cAMP are thought to open the same intracellular gate (75, 87). The gate must be coupled to both the voltage sensors and the CNBD for the channel to open in response to these stimuli. The mechanism of SpIH inactivation is thought to involve a "slip," or uncoupling, of the voltage sensors and the activation gate. Binding of cAMP must be able to prevent the channel from "slipping," as cAMP removes inactivation (75). SpIH can be thought of as functionally intermediate between HCN and CNG channels. SpIH channels are activated by hyperpolarization, as are HCN channels, but binding of cyclic nucleotides drastically increases the open probability of SpIH channels, as with CNG channels. These comparisons are especially apparent when looking at eletrophysiological data from all three types of channels, as in Figure 10.

EFFECTS OF CYCLIC NUCLEOTIDES ON CNG CHANNELS In the absence of cyclic nucleotide, the open probability of CNG channels is extremely low (10^{-4}–10^{-6}) (88, 89). In CNGA1 channels, cGMP dramatically increases the open probability, whereas inosine 3′,5′-cyclic monophosphate (cIMP) and cAMP increase the open probability less (Figure 10). The change in free energy of CNG channel opening in the presence of cyclic nucleotides relative to unliganded channel opening, $\Delta\Delta G$, can be estimated for each ligand. If the free energy of opening for unliganded channels is 6.8 kcal mol^{-1} ($\Delta G = -RTlnL$, where the equilibrium constant for channel opening $L = 1 \times 10^{-5}$), the $\Delta\Delta G$ values for each ligand are -8.8 kcal mol^{-1} for cGMP, −6.9 kcal mol^{-1} for cIMP, and −3.9 kcal mol^{-1} for cAMP (ΔG values from Reference 90). The $\Delta\Delta G$ values for cAMP are similar for CNGA1 and HCN2. cGMP, however, is a better agonist than cAMP for CNGA1 channels. This differential activation by agonists is observed in other CNG channels, although the relative effects of the different cyclic nucleotides are not always the same (74, 91–93). All of the cyclic nucleotides are thought to open the same activation gate in CNG channels, which is thought to be located in the pore loop, not intracellularly as it is in HCN and SpIH channels (94–97).

The greater agonist efficacy of cGMP in CNG channels is thought to be due, at least partially, to a residue in the C-helix that corresponds to Ile636 in HCN2. This residue interacts with cAMP in the HCN2 C-terminal crystal structure. If this residue, Asp604 of CNGA1, is mutated to a neutral residue, the channel's agonist selectivity switches from preferring cGMP to preferring cAMP (93, 98). These results suggest that Asp604 is hydrogen bonding to the N_1 and N_2 amines of the guanine ring of cGMP. Additionally, the high cGMP affinity of CNG channels is thought to arise from hydrogen bonding of Thr560 of CNGA1 with the N_2 amine of cGMP (84), as shown in the HCN2 C-terminal crystal structure (73). Therefore, it is possible that Thr560 holds cGMP in the syn configuration during initial binding

and that Asp604 then interacts with cGMP during the allosteric conformational change of channel opening. Owing to the conservation of residues that interact with ligand in CNG and HCN channels, cyclic nucleotides probably bind in the same configuration in both channels.

MUTATIONS WITH SIMILAR EFFECTS ON CNG AND HCN CYCLIC NUCLEOTIDE MODULATION If cyclic nucleotides activate CNG and HCN channels in a similar manner, then mutations that affect cyclic nucleotide modulation would be predicted to have similar effects on CNG and HCN channel behavior. As discussed above, the crystal structure of the HCN2 C-terminal region shows various intersubunit interactions, primarily in the C-linker regions, in which the A′ and B′ "elbow" of one subunit rests on the C′ and D′ "shoulder" of its neighbor (Figure 8). As these interactions are the points of subunit contact and are in the C-linker, they may assist in conferring ligand binding to the pore, resulting in channel opening. The crystal structure contains two salt bridges per subunit in the "elbow on the shoulder" region: one between the B′-helix and the D′-helix of the neighboring subunit (intersubunit salt bridge) and one between the same B′-helix residue and the β-roll of the same subunit (intrasubunit salt bridge). Mutation of these salt bridges revealed that they are present in intact HCN2 channels and in CNGA1 channels as well (67). Surprisingly, disruption of these salt bridges through mutation favors channel opening in both CNG and HCN channels. These results suggest that the C-linkers are in the closed configuration even though the CNBD is ligand bound in the HCN2 C-terminal crystal structure. Moreover, these findings highlight both the modular nature of gating as well as similarities between CNG and HCN channel structure and behavior.

Another recent result that suggests similar cyclic nucleotide modulation for CNG and HCN channels is the finding that three amino acids in the C-linker are crucial for normal ligand efficacy (74). This tripeptide is conserved among CNGA1, CNGA2, CNGA3, and HCN subunits, but not among CNGA4, CNGB1, or CNGB3 (channels that cannot produce functional homomers). If the C-linker of CNGA2 channels is substituted into CNGA4 channels, these chimeras are able to form functional homomers. When the conserved tripeptide is substituted with a tripeptide from CNGA4 in HCN channels, the efficacy of cAMP is greatly reduced. In fact, in this mutant, cAMP seems to inhibit rather than favor channel opening, as it does normally. Thus, it is suggested that this tripeptide confers the normal increase in open probability, with cyclic nucleotide binding in both CNG and HCN channels.

POSSIBLE MECHANISMS OF ACTIVATION BY CYCLIC NUCLEOTIDES

Understanding gating has long been a goal of ion channel research, and hence there have been numerous proposed mechanisms. Over time, and with advances in understanding of CNG and HCN channel behavior, quite a few mechanisms

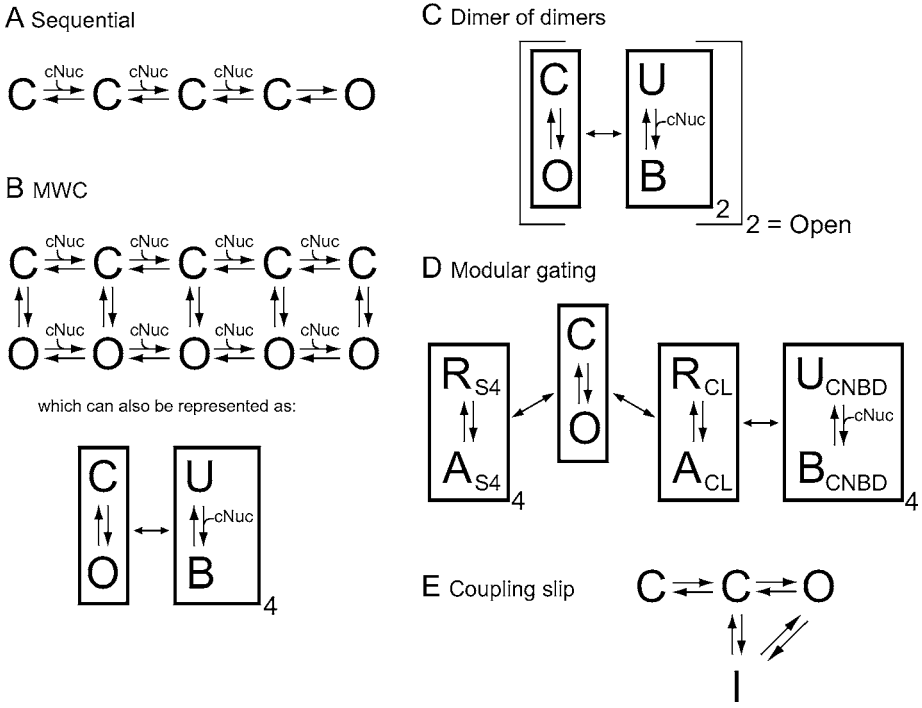

Figure 11 Proposed activation mechanisms (*A–E*) for CNG and HCN channels. States are shown as closed (C), open (O), resting (R), activated (A), unbound (U), and bound with ligand (B). Boxes around states indicate separable gating modules. Single-headed arrows indicate equilibrium between states, and double-headed arrows indicate coupling between gating modules.

have been suggested. The models that have been suggested to explain cyclic nucleotide activation of CNG and HCN channels are the sequential model; the Monod, Wyman, and Changeux (MWC) model; the dimer-of-dimers model; the modular gating model; and the coupling slip model (Figure 11).

The simplest model to explain cyclic nucleotide modulation is the sequential model. Originally formulated to describe retinal rod CNG channel response to increasing cyclic nucleotide concentration and voltage, the sequential model allows for sequential cyclic nucleotide–binding steps to closed channels, followed by a final closed-to-open transition when the channel is fully liganded (Figure 11*A*) (99). Variations of this model involving two to four ligand-binding steps have been proposed (99, 100). The two channel states, closed and open, are assumed to be the only conductance states. Additionally, the model assumes that the closed-to-open transition is very rapid and weakly voltage dependent. This model can reproduce the kinetic and steady-state behavior of CNG channels in response to various cyclic nucleotide concentrations and permits effects on ligand binding

to be separated from effects on channel opening. However, this model does not completely reproduce channel behavior because it does not allow for channels to open when they are unliganded or partially liganded. Because CNG channels do show unliganded openings (89), and HCN channels open very well without ligand, this model is insufficient.

The next progression of modeling was the MWC model, a classic allosteric model that was originally formulated to describe hemoglobin behavior (101). The MWC model has been invoked to explain the dual activation by voltage and cyclic nucleotides for both CNG and HCN channels (89, 102–104). Generally, the MWC model is a gating scheme in which a concerted conformational transition occurs from the closed to the open state of the channel, and this transition is energetically stabilized by a constant amount for each ligand bound. This model therefore explicitly allows for opening to occur whether the channel is unliganded, partially liganded, or fully liganded (Figure 11*B*). Thus, at saturating concentrations of ligand, all four binding sites are assumed to be occupied and the model is reduced to one in which the channel is either closed but fully liganded or open and fully liganded. This is reminiscent of the final closed-to-open transition of the sequential model. The MWC model reproduces both the voltage dependence and the modulation of cyclic nucleotides for both HCN and CNG channels. However, the model is limited by the assumptions that there are four identical binding sites and that channel opening can be reduced to a single concerted allosteric transition of the entire protein.

In order to address these limitations of the MWC model, two different models have been proposed: a dimer-of-dimers model (Figure 11*C*) and modular gating model (Figure 11*D*). The dimer-of-dimers model arose from experiments designed to discover the energetic contribution of binding successive ligands to CNG and HCN channels (78, 105). In this model, each dimer acts as an MWC unit that undergoes a concerted allosteric transition from closed to open, but both dimers must be open for the channel to be open. This model suggests that in the absence of ligand, the C-terminal region assembles into a twofold symmetry and does not favor channel opening. Once the channel opens, it is thought to recover fourfold symmetry, as seen in the HCN2 crystal structure. Addition of cyclic nucleotide promotes channel opening and thus promotes fourfold symmetry. This model explains the energetic contribution of binding successive ligands in CNG and HCN channels.

The modular gating model arose from evidence that ion channels seem to undergo a series of coupled conformational changes in separate domains of the channel (106). This is in contrast to the single allosteric transition of the entire channel that is assumed by the MWC model. Cyclic nucleotide–dependent activation of CNG and HCN channels can be described as interactions between four domains: the pore, the S4 voltage sensor, the C-linker, and the CNBD (Figure 11*D*). Each domain, or module, is in equilibrium between two possible conformations. The pore can be closed or open, the voltage sensor and the C-linker can be resting or activated, and the CNBD can be unbound or bound with ligand. The modules are then coupled to each other, indicating that the conformation of one module affects the conformation of another module. This model can simulate the voltage

dependence and cyclic nucleotide modulation for both HCN2 and CNGA1 channels (67).

In addition to reproducing voltage dependence and cyclic nucleotide modulation for both CNG and HCN channels, the modular gating model may also explain how, in the HCN2 C-terminal crystal structure, the CNBD can be bound by ligand while the C-linker can be in its resting conformation. If the resting state of the C-linker normally has an inhibitory effect on pore opening, then removing the pore (as for the HCN2 C-terminal crystal structure) should promote the resting state of the C-linker. Therefore, even in the presence of ligand, the "unloaded" (isolated from the pore) C-linker may return to its resting state. In fact, inhibition by the C-terminal regions has been proposed in a study with C-terminal deletion mutants of HCN1 and HCN2 channels (69). The CNBD exerts an inhibitory effect on channel activation by shifting the V_{half} of channel activation to more hyperpolarized potentials. Thus the modular gating model is a plausible model to explain HCN and CNG channel behavior.

A final model that has been proposed for HCN channels is the coupling slip model (Figure 11*E*). This model was proposed to explain the occurrence of inactivation in SpIH (and HCN) channels in the absence of cAMP (75). This model incorporates the idea that the voltage sensor and the activation gate are coupled and that, in the absence of cyclic nucleotide in SpIH, this coupling can "slip" such

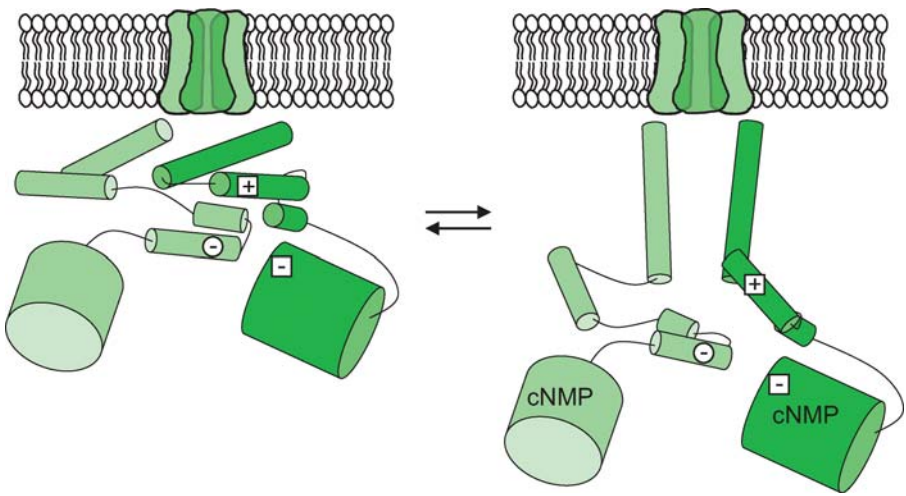

Figure 12 Gating model. Depiction of the HCN2 C-terminal regions from the side view, both in the resting configuration (*left*) and the active configuration (*right*). C-terminal regions of two subunits (*dark* and *light green*) are shown below the membrane-spanning portion of the channel. α-helices are shown with narrow cylinders, and the β-rolls of the CNBDs with wide cylinders. Salt bridge residues are shown: the positive B′-helix residue (*plus sign within square*) and the two negative residues on the D′-helix and the β-roll (*minus sign within circle* and *minus sign within square*).

that the channel will close even though the voltage sensor is activated, producing inactivation. In the presence of cyclic nucleotide, a coupling slip does not occur. A combination of the coupling slip model and the modular gating model may prove useful to predict behavior of CNG, HCN, and SpIH channels.

Using the modular gating scheme and conclusions derived from various CNG and HCN channel experiments, we can construct a cartoon demonstrating how these channels respond to cyclic nucleotide binding (Figure 12). In the absence of ligand, the C-linker is thought to be in a compact state, perhaps held in this position by "elbow on the shoulder" interactions, including salt bridges, between neighboring subunits and intrasubunit interactions between C-linkers and CNBDs. This compact state produces an inhibitory effect on channel opening. Then cyclic nucleotide binds to the CNBD, and there must be a quaternary rearrangement of the C-linkers, which removes the inhibitory effect of the C-terminal region. The C-terminal ends of the CNG S6 segments, which connect to the N-terminal ends of the A′-helices, are thought to be close together when the channel is closed and further apart when the channel is open (96, 107). Additionally, several His residues in the CNGA1 A′-helix, for example H420, are able to coordinate Ni^{2+} between the same residue on neighboring subunits in the open state of the channel (100, 108). In order for the A′-helices to be able to coordinate Ni^{2+}, the C-linkers must move such that the C-terminal ends of the A′-helices move closer together toward the central axis of the channel. This relaxed structure would disrupt the salt bridges that hold the C-terminal region in the tense structure, favoring channel opening.

CONCLUSIONS

Through structure-function analysis of CNG and HCN channels, a number of mechanisms have been proposed to explain gating and modulation by cyclic nucleotides. Initially these mechanisms only focused on certain features of channel behavior, such as liganded channel openings, and did not account for more complex behaviors, such as unliganded (spontaneous) openings and voltage-dependent openings. But as more was learned about these channels, the mechanisms became more elaborate. These latest mechanisms can apply to both CNG and HCN channels, two peas in a pod.

The *Annual Review of Physiology* is online at
http://physiol.annualreviews.org

LITERATURE CITED

1. Hille B. 2001. *Ion Channels of Excitable Membranes*. Sunderland, MA: Sinhauer Assoc., Inc. 814 pp.
2. Fesenko EE, Kolesnikov SS, Lyubarsky AL. 1985. Induction by cyclic GMP of cationic conductance in plasma membrane of retinal rod outer segment. *Nature* 313:310–13

3. Kaupp UB, Seifert R. 2002. Cyclic nucleotide-gated ion channels. *Physiol. Rev.* 82:769–824
4. Matulef K, Zagotta WN. 2003. Cyclic nucleotide-gated ion channels. *Annu. Rev. Cell Dev. Biol.* 19:23–44
5. Burns ME, Baylor DA. 2001. Activation, deactivation, and adaptation in vertebrate photoreceptor cells. *Annu. Rev. Neurosci.* 24:779–805
6. Detwiler P. 2002. Open the loop: Dissecting feedback regulation of a second messenger transduction cascade. *Neuron* 36:3–4
7. Palczewski K, Sokal I, Baehr W. 2004. Guanylate cyclase-activating proteins: Structure, function, and diversity. *Biochem. Biophys. Res. Commun.* 322:1123–30
8. Sharma RK. 2002. Evolution of the membrane guanylate cyclase transduction system. *Mol. Cell. Biochem.* 230:3–30
9. Frings S. 2001. Chemoelectrical signal transduction in olfactory sensory neurons of air-breathing vertebrates. *Cell. Mol. Life Sci.* 58:510–19
10. Bradley J, Reuter D, Frings S. 2001. Facilitation of calmodulin-mediated odor adaptation by cAMP-gated channel subunits. *Science* 294:2176–78
11. Chen TY, Yau KW. 1994. Direct modulation by Ca^{2+}-calmodulin of cyclic nucleotide-activated channel of rat olfactory receptor neurons. *Nature* 368:545–48
12. Kurahashi T, Menini A. 1997. Mechanism of odorant adaptation in the olfactory receptor cell. *Nature* 385:725–29
13. Munger SD, Lane AP, Zhong H, Leinders-Zufall T, Yau KW, et al. 2001. Central role of the CNGA4 channel subunit in Ca^{2+}-calmodulin-dependent odor adaptation. *Science* 294:2172–75
14. Weitz D, Ficek N, Kremmer E, Bauer PJ, Kaupp UB. 2002. Subunit stoichiometry of the CNG channel of rod photoreceptors. *Neuron* 36:881–89
15. Zheng J, Trudeau MC, Zagotta WN. 2002. Rod cyclic nucleotide-gated channels have a stoichiometry of three CNGA1 subunits and one CNGB1 subunit. *Neuron* 36:891–96
16. Zhong H, Molday LL, Molday RS, Yau KW. 2002. The heteromeric cyclic nucleotide-gated channel adopts a 3A:1B stoichiometry. *Nature* 420:193–98
17. Peng C, Rich ED, Varnum MD. 2004. Subunit configuration of heteromeric cone cyclic nucleotide-gated channels. *Neuron* 42:401–10
18. Zheng J, Zagotta WN. 2004. Stoichiometry and assembly of olfactory cyclic nucleotide-gated channels. *Neuron* 42:411–21
19. Accili EA, Redaelli G, DiFrancesco D. 1997. Differential control of the hyperpolarization-activated current (i(f)) by cAMP gating and phosphatase inhibition in rabbit sino-atrial node myocytes. *J. Physiol.* 500(Pt. 3):643–51
20. DiFrancesco D. 1986. Characterization of single pacemaker channels in cardiac sino-atrial node cells. *Nature* 324:470–73
21. DiFrancesco D. 1991. The contribution of the "pacemaker" current (if) to generation of spontaneous activity in rabbit sino-atrial node myocytes. *J. Physiol.* 434:23–40
22. Dokos S, Celler B, Lovell N. 1996. Ion currents underlying sinoatrial node pacemaker activity: A new single cell mathematical model. *J. Theor. Biol.* 181:245–72
23. Stieber J, Hofmann F, Ludwig A. 2004. Pacemaker channels and sinus node arrhythmia. *Trends Cardiovasc. Med.* 14:23–28
24. Altomare C, Terragni B, Brioschi C, Milanesi R, Pagliuca C, et al. 2003. Heteromeric HCN1-HCN4 channels: A comparison with native pacemaker channels from the rabbit sinoatrial node. *J. Physiol.* 549:347–59
25. Guth BD, Dietze T. 1995. I(f) current mediates beta-adrenergic enhancement of heart rate but not contractility in vivo. *Basic Res. Cardiol.* 90:192–202

26. Mangoni ME, Nargeot J. 2001. Properties of the hyperpolarization-activated current (I(f)) in isolated mouse sino-atrial cells. *Cardiovasc. Res*. 52:51–64
27. Ono K, Shibata S, Iijima T. 2003. Pacemaker mechanism of porcine sino-atrial node cells. *J. Smooth Muscle Res.* 39:195–204
28. Stein RB, Gossen ER, Jones KE. 2005. Neuronal variability: Noise or part of the signal? *Nat. Rev. Neurosci*. 6:389–97
29. Chan CS, Shigemoto R, Mercer JN, Surmeier DJ. 2004. HCN2 and HCN1 channels govern the regularity of autonomous pacemaking and synaptic resetting in globus pallidus neurons. *J. Neurosci*. 24:9921–32
30. Banks MI, Pearce RA, Smith PH. 1993. Hyperpolarization-activated cation current (Ih) in neurons of the medial nucleus of the trapezoid body: voltage-clamp analysis and enhancement by norepinephrine and cAMP suggest a modulatory mechanism in the auditory brain stem. *J. Neurophysiol*. 70:1420–32
31. Cuttle MF, Rusznak Z, Wong AY, Owens S, Forsythe ID. 2001. Modulation of a presynaptic hyperpolarization-activated cationic current (I(h)) at an excitatory synaptic terminal in the rat auditory brainstem. *J. Physiol*. 534:733–44
32. Ingram SL, Williams JT. 1996. Modulation of the hyperpolarization-activated current (Ih) by cyclic nucleotides in guinea-pig primary afferent neurons. *J. Physiol*. 492(Pt. 1):97–106
33. Saitow F, Konishi S. 2000. Excitability increase induced by beta-adrenergic receptor-mediated activation of hyperpolarization-activated cation channels in rat cerebellar basket cells. *J. Neurophysiol*. 84:2026–34
34. Moosmang S, Stieber J, Zong X, Biel M, Hofmann F, Ludwig A. 2001. Cellular expression and functional characterization of four hyperpolarization-activated pacemaker channels in cardiac and neuronal tissues. *Eur. J. Biochem*. 268:1646–52
35. Lujan R, Albasanz JL, Shigemoto R, Juiz JM. 2005. Preferential localization of the hyperpolarization-activated cyclic nucleotide-gated cation channel subunit HCN1 in basket cell terminals of the rat cerebellum. *Eur. J. Neurosci*. 21:2073–82
36. Magee JC. 1999. Dendritic lh normalizes temporal summation in hippocampal CA1 neurons. *Nat. Neurosci*. 2:508–14
37. Williams SR, Stuart GJ. 2000. Site independence of EPSP time course is mediated by dendritic I(h) in neocortical pyramidal neurons. *J. Neurophysiol*. 83:3177–82
38. Moosmang S, Biel M, Hofmann F, Ludwig A. 1999. Differential distribution of four hyperpolarization-activated cation channels in mouse brain. *Biol. Chem*. 380:975–80
39. Santoro B, Chen S, Luthi A, Pavlidis P, Shumyatsky GP, et al. 2000. Molecular and functional heterogeneity of hyperpolarization-activated pacemaker channels in the mouse CNS. *J. Neurosci*. 20:5264–75
40. Baruscotti M, Difrancesco D. 2004. Pacemaker channels. *Ann. NY Acad. Sci*. 1015:111–21
41. Tang CY, Papazian DM. 1997. Transfer of voltage independence from a rat olfactory channel to the Drosophila ether-a-go-go K^+ channel. *J. Gen. Physiol*. 109:301–11
42. Doyle DA, Morais Cabral J, Pfuetzner RA, Kuo A, Gulbis JM, et al. 1998. The structure of the potassium channel: Molecular basis of K^+ conduction and selectivity. *Science* 280:69–77
43. Trudeau MC, Zagotta WN. 2003. Calcium/calmodulin modulation of olfactory and rod cyclic nucleotide-gated ion channels. *J. Biol. Chem*. 278:18705–8
44. Zhong H, Lai J, Yau KW. 2003. Selective heteromeric assembly of cyclic nucleotide-gated channels. *Proc. Natl. Acad. Sci. USA* 100:5509–13
45. Bruggemann A, Pardo LA, Stuhmer W, Pongs O. 1993. Ether-a-go-go encodes a voltage-gated channel permeable to K^+

and Ca^{2+} and modulated by cAMP. *Nature* 365:445–48
46. Cui J, Melman Y, Palma E, Fishman GI, McDonald TV. 2000. Cyclic AMP regulates the HERG K^+ channel by dual pathways. *Curr. Biol*. 10:671–74
47. Hoshi T. 1995. Regulation of voltage dependence of the KAT1 channel by intracellular factors. *J. Gen. Physiol*. 105: 309–28
48. Eismann E, Muller F, Heinemann SH, Kaupp UB. 1994. A single negative charge within the pore region of a cGMP-gated channel controls rectification, Ca^{2+} blockage, and ionic selectivity. *Proc. Natl. Acad. Sci. USA* 91:1109–13
49. Heinemann SH, Terlau H, Stuhmer W, Imoto K, Numa S. 1992. Calcium channel characteristics conferred on the sodium channel by single mutations. *Nature* 356:441–43
50. Hess P, Lansman JB, Tsien RW. 1986. Calcium channel selectivity for divalent and monovalent cations. Voltage and concentration dependence of single channel current in ventricular heart cells. *J. Gen. Physiol*. 88:293–319
51. Sesti F, Eismann E, Kaupp UB, Nizzari M, Torre V. 1995. The multi-ion nature of the cGMP-gated channel from vertebrate rods. *J. Physiol*. 487(Pt. 1):17–36
52. Yang J, Ellinor PT, Sather WA, Zhang JF, Tsien RW. 1993. Molecular determinants of Ca^{2+} selectivity and ion permeation in L-type Ca^{2+} channels. *Nature* 366:158–61
53. Heginbotham L, Abramson T, MacKinnon R. 1992. A functional connection between the pores of distantly related ion channels as revealed by mutant K^+ channels. *Science* 258:1152–55
54. Ludwig A, Zong X, Jeglitsch M, Hofmann F, Biel M. 1998. A family of hyperpolarization-activated mammalian cation channels. *Nature* 393:587–91
55. Proenza C, Angoli D, Agranovich E, Macri V, Accili EA. 2002. Pacemaker channels produce an instantaneous current. *J. Biol. Chem*. 277:5101–9
56. DiFrancesco D. 1981. A new interpretation of the pace-maker current in calf Purkinje fibres. *J. Physiol*. 314:359–76
57. Dzeja C, Hagen V, Kaupp UB, Frings S. 1999. Ca^{2+} permeation in cyclic nucleotide-gated channels. *EMBO J*. 18: 131–44
58. Yu X, Duan KL, Shang CF, Yu HG, Zhou Z. 2004. Calcium influx through hyperpolarization-activated cation channels (I(h) channels) contributes to activity-evoked neuronal secretion. *Proc. Natl. Acad. Sci. USA* 101:1051–56
59. Biel M, Schneider A, Wahl C. 2002. Cardiac HCN channels: Structure, function, and modulation. *Trends Cardiovasc. Med.* 12:206–12
60. Mannikko R, Elinder F, Larsson HP. 2002. Voltage-sensing mechanism is conserved among ion channels gated by opposite voltages. *Nature* 419:837–41
61. Vemana S, Pandey S, Larsson HP. 2004. S4 movement in a mammalian HCN channel. *J. Gen. Physiol*. 123:21–32
62. Bell DC, Yao H, Saenger RC, Riley JH, Siegelbaum SA. 2004. Changes in local S4 environment provide a voltage-sensing mechanism for mammalian hyperpolarization-activated HCN channels. *J. Gen. Physiol*. 123:5–19
63. Aggarwal SK, MacKinnon R. 1996. Contribution of the S4 segment to gating charge in the Shaker K^+ channel. *Neuron* 16:1169–77
64. Schoppa NE, McCormack K, Tanouye MA, Sigworth FJ. 1992. The size of gating charge in wild-type and mutant Shaker potassium channels. *Science* 255:1712–15
65. Zagotta WN, Hoshi T, Dittman J, Aldrich RW. 1994. Shaker potassium channel gating. II: Transitions in the activation pathway. *J. Gen. Physiol*. 103:279–319
66. Chen S, Wang J, Siegelbaum SA. 2001. Properties of hyperpolarization-activated pacemaker current defined by coassembly

of HCN1 and HCN2 subunits and basal modulation by cyclic nucleotide. *J. Gen. Physiol*. 117:491–504
67. Craven KB, Zagotta WN. 2004. Salt bridges and gating in the COOH-terminal region of HCN2 and CNGA1 channels. *J. Gen. Physiol*. 124:663–77
68. Ludwig A, Zong X, Stieber J, Hullin R, Hofmann F, Biel M. 1999. Two pacemaker channels from human heart with profoundly different activation kinetics. *EMBO J*. 18:2323–29
69. Wainger BJ, DeGennaro M, Santoro B, Siegelbaum SA, Tibbs GR. 2001. Molecular mechanism of cAMP modulation of HCN pacemaker channels. *Nature* 411: 805–10
70. Wang J, Chen S, Nolan MF, Siegelbaum SA. 2002. Activity-dependent regulation of HCN pacemaker channels by cyclic AMP: Signaling through dynamic allosteric coupling. *Neuron* 36:451–61
71. Wang J, Chen S, Siegelbaum SA. 2001. Regulation of hyperpolarization-activated HCN channel gating and cAMP modulation due to interactions of COOH terminus and core transmembrane regions. *J. Gen. Physiol*. 118:237–50
72. Yu HG, Lu Z, Pan Z, Cohen IS. 2004. Tyrosine kinase inhibition differentially regulates heterologously expressed HCN channels. *Pflugers Arch.* 447:392–400
73. Zagotta WN, Olivier NB, Black KD, Young EC, Olson R, Gouaux E. 2003. Structural basis for modulation and agonist specificity of HCN pacemaker channels. *Nature* 425:200–5
74. Zhou L, Olivier NB, Yao H, Young EC, Siegelbaum SA. 2004. A conserved tripeptide in CNG and HCN channels regulates ligand gating by controlling C-terminal oligomerization. *Neuron* 44:823–34
75. Shin KS, Maertens C, Proenza C, Rothberg BS, Yellen G. 2004. Inactivation in HCN channels results from reclosure of the activation gate: Desensitization to voltage. *Neuron* 41:737–44
76. Shin KS, Rothberg BS, Yellen G. 2001. Blocker state dependence and trapping in hyperpolarization-activated cation channels: Evidence for an intracellular activation gate. *J. Gen. Physiol.* 117:91–101
77. Tibbs GR, Liu DT, Leypold BG, Siegelbaum SA. 1998. A state-independent interaction between ligand and a conserved arginine residue in cyclic nucleotide-gated channels reveals a functional polarity of the cyclic nucleotide binding site. *J. Biol. Chem*. 273:4497–505
78. Ulens C, Siegelbaum SA. 2003. Regulation of hyperpolarization-activated HCN channels by cAMP through a gating switch in binding domain symmetry. *Neuron* 40:959–70
79. Kim LA, Furst J, Gutierrez D, Butler MH, Xu S, et al. 2004. Three-dimensional structure of I_{to}; Kv4.2-KChIP2 ion channels by electron microscopy at 21 Angstrom resolution. *Neuron* 41:513–19
80. Sokolova O, Kolmakova-Partensky L, Grigorieff N. 2001. Three-dimensional structure of a voltage-gated potassium channel at 2.5 nm resolution. *Structure* 9:215–20
81. Johnson JP Jr, Zagotta WN. 2005. The carboxyl-terminal region of cyclic nucleotide-modulated channels is a gating ring, not a permeation path. *Proc. Natl. Acad. Sci. USA* 102:2742–47
82. Su Y, Dostmann WR, Herberg FW, Durick K, Xuong NH, et al. 1995. Regulatory subunit of protein kinase A: Structure of deletion mutant with cAMP binding domains. *Science* 269:807–13
83. Weber IT, Gilliland GL, Harman JG, Peterkofsky A. 1987. Crystal structure of a cyclic AMP-independent mutant of catabolite gene activator protein. *J. Biol. Chem*. 262:5630–36
84. Altenhofen W, Ludwig J, Eismann E, Kraus W, Bonigk W, Kaupp UB. 1991. Control of ligand specificity in cyclic nucleotide-gated channels from rod photoreceptors and olfactory epithelium. *Proc. Natl. Acad. Sci. USA* 88:9868–72

85. DiFrancesco D, Tortora P. 1991. Direct activation of cardiac pacemaker channels by intracellular cyclic AMP. *Nature* 351:145–47
86. Gauss R, Seifert R, Kaupp UB. 1998. Molecular identification of a hyperpolarization-activated channel in sea urchin sperm. *Nature* 393:583–87
87. Rothberg BS, Shin KS, Phale PS, Yellen G. 2002. Voltage-controlled gating at the intracellular entrance to a hyperpolarization-activated cation channel. *J. Gen. Physiol*. 119:83–91
88. Ruiz ML, Karpen JW. 1997. Single cyclic nucleotide-gated channels locked in different ligand-bound states. *Nature* 389:389–92
89. Tibbs GR, Goulding EH, Siegelbaum SA. 1997. Allosteric activation and tuning of ligand efficacy in cyclic-nucleotide-gated channels. *Nature* 386:612–15
90. Sunderman ER, Zagotta WN. 1999. Mechanism of allosteric modulation of rod cyclic nucleotide-gated channels. *J. Gen. Physiol*. 113:601–20
91. Gordon SE, Zagotta WN. 1995. Localization of regions affecting an allosteric transition in cyclic nucleotide-activated channels. *Neuron* 14:857–64
92. Shapiro MS, Zagotta WN. 2000. Structural basis for ligand selectivity of heteromeric olfactory cyclic nucleotide-gated channels. *Biophys. J*. 78:2307–20
93. Varnum MD, Black KD, Zagotta WN. 1995. Molecular mechanism for ligand discrimination of cyclic nucleotide-gated channels. *Neuron* 15:619–25
94. Becchetti A, Gamel K, Torre V. 1999. Cyclic nucleotide-gated channels. Pore topology studied through the accessibility of reporter cysteines. *J. Gen. Physiol*. 114:377–92
95. Becchetti A, Roncaglia P. 2000. Cyclic nucleotide-gated channels: Intra- and extracellular accessibility to Cd^{2+} of substituted cysteine residues within the P-loop. *Pflugers Arch*. 440:556–65
96. Flynn GE, Zagotta WN. 2001. Conformational changes in S6 coupled to the opening of cyclic nucleotide-gated channels. *Neuron* 30:689–98
97. Liu J, Siegelbaum SA. 2000. Change of pore helix conformational state upon opening of cyclic nucleotide-gated channels. *Neuron* 28:899–909
98. Sunderman ER, Zagotta WN. 1999. Sequence of events underlying the allosteric transition of rod cyclic nucleotide-gated channels. *J. Gen. Physiol*. 113:621–40
99. Karpen JW, Zimmerman AL, Stryer L, Baylor DA. 1988. Gating kinetics of the cyclic-GMP-activated channel of retinal rods: Flash photolysis and voltage-jump studies. *Proc. Natl. Acad. Sci. USA* 85:1287–91
100. Gordon SE, Zagotta WN. 1995. Subunit interactions in coordination of Ni^{2+} in cyclic nucleotide-gated channels. *Proc. Natl. Acad. Sci. USA* 92:10222–26
101. Monod J, Wyman J, Changeux JP. 1965. On the nature of allosteric transitions: A plausible model. *J. Mol. Biol*. 12:88–118
102. DiFrancesco D. 1999. Dual allosteric modulation of pacemaker (f) channels by cAMP and voltage in rabbit SA node. *J. Physiol*. 515(Pt. 2):367–76
103. Goulding EH, Tibbs GR, Siegelbaum SA. 1994. Molecular mechanism of cyclic-nucleotide-gated channel activation. *Nature* 372:369–74
104. Varnum MD, Zagotta WN. 1996. Subunit interactions in the activation of cyclic nucleotide-gated ion channels. *Biophys. J*. 70:2667–79
105. Liu DT, Tibbs GR, Paoletti P, Siegelbaum SA. 1998. Constraining ligand-binding site stoichiometry suggests that a cyclic nucleotide-gated channel is composed of two functional dimers. *Neuron* 21:235–48
106. Horrigan FT, Aldrich RW. 2002. Coupling between voltage sensor activation,

Ca^{2+} binding and channel opening in large conductance (BK) potassium channels. *J. Gen. Physiol.* 120:267–305

107. Flynn GE, Zagotta WN. 2003. A cysteine scan of the inner vestibule of cyclic nucleotide-gated channels reveals architecture and rearrangement of the pore. *J. Gen. Physiol.* 121:563–82
108. Johnson JP Jr, Zagotta WN. 2001. Rotational movement during cyclic nucleotide-gated channel opening. *Nature* 412: 917–21

Annual Review of Physiology
Volume 68, 2006

CONTENTS